Datashare 70:

Hydrogen sulfide formation, fate, and behavior in anhydrite-sealed carbonate gas reservoirs: A three-dimensional reactive mass transport modeling approach

Yunjiao Fu, Wolfgang van Berk, and Hans-Martin Schulz

AAPG Bulletin, v. 100, no. 5 (May 2016), pp. 843–865

Appendix 1: Reservoir Properties and Thermodynamic Data

To reproduce a reservoir structure, the simulated reservoir analogy comprises a seal, a gas cap, a gas–water transition zone, and a water leg (Figure 2, Table S.1). The water leg shows a thickness of 50 m (164 ft) (1000 × 2 × 50 m [3280 × 7 × 164 ft] in X, Y, and Z directions). The gas–water transition zone consists of two thin layers: (1) from 100 to 900 m (328 to 2953 ft) in X direction, from 0 to 2 m (0 to 7 ft) in Y direction, and from 50 to 52 m (164 to 171 ft) in Z direction; (2) from 200 to 800 m (656 to 2625 ft) in X direction, from 0 to 2 m (0 to 7 ft) in Y direction, and from 52 to 53 m (171 to 174 ft) in Z direction (Figure 2). Thus, the transition zone has a thickness of 2 to 3 m (7 to 10 ft) in the Z direction (Table S.1). The gas cap has four layers: (1) from 200 to 800 m (656 to 2625 ft) in X direction, from 0 to 2 m (0 to 7 ft) in Y direction, and from 53 to 55 m (174 to 180 ft) in Z direction; (2) from 300 to 700 m (984 to 2297 ft) in X direction, from 0 to 2 m (0 to 7 ft) in Y direction, and from 55 to 59 m (180 to 194 ft) in Z direction; (3) from 350 to 650 m (1148 to 2133 ft) in X direction, from 0 to 2 m (0 to 7 ft) in Y direction, and from 59 to 62 m (194 to 203 ft) in Z direction; and (4) from 400 to 600 m (1312 to 1969 ft) in X direction, from 0 to 2 m (0 to 7 ft) in Y direction, and from 62 to 65 m (203 to 213 ft) in Z direction (Figure 2). The remaining part is the seal (Figure 2). The four reservoir parts (seal, gas cap, gas–water transition zone, water leg) are characterized by different physical and geochemical properties (Tables S.1–S.3). The hydraulic conductivity and dispersivity (Table S.1) for each part are arbitrarily predefined. However, such predefined values have no effect on the modeling results, because diffusion is the only transport process considered in our model. The model applies a molecular diffusivity of 10^{-9} m^2 s^{-1} as a scalar value that is constant over the entire grid region and valid for all $\text{species}_{(aq)}$. Due to their different properties (e.g., water content), these four reservoir parts are characterized by different intensities of diffusive mass transport. Our model images this effect by using a decreasing tortuosity from the water leg to the seal (1.0, 0.5, 0.1, and 0.01 in scenario 1–reference, respectively; Table S.1). Diffusive mass exchange is allowed within all reservoir parts, while the model boundaries are defined by closed boundary conditions.

The mineralogical composition of the reservoir rocks and the seal are also assumed and defined as mole per liter pore (or irreducible) water in the input file (Table S.2). For this, the density of all primary minerals is taken from Dean (1999): 2.96 g cm^{-3} for anhydrite, 2.711 g cm^{-3} for calcite, 2.872 g cm^{-3} for dolomite, and 4.26 g cm^{-3} for goethite. Anhydrite (99 wt. %) dominates in the seal which additionally comprises 1 wt. % calcite. The rock matrices of the gas cap, the gas–water transition zone and the water leg show an identical mineralogical composition: 10 wt. % calcite, 89 wt. % dolomite, and 1 wt. % goethite. The amount of all primary minerals (anhydrite, calcite, dolomite, and goethite) is converted from wt. % with consideration of the porosity saturated with pore (irreducible) water and of the density of these minerals into the unit of mol kgw^{-1} (for details, see Table S.2). Before the onset of abiotic sulfate reduction (ASR), a gas phase with an assumed composition prevails in the gas cap: 97 vol. % $CH_{4(g)}$ and 3 vol. % $CO_{2(g)}$ under the reservoir pressure of 600 atm (8818 psi) (equal to 582 and 18 atm [8553 and 265 psi], respectively; Table S.2).

Our study considers a semigeneric reservoir which mineralogical and gas composition are assumed. According to the both parameters, the pore (or irreducible) water composition in each reservoir part is calculated by equilibrating a 1.5 molal NaCl solution with the primary minerals or gases present under initial conditions (before the ASR onset; Table S.2). This separate calculation was performed by the computer code PHREEQC (Parkhurst and Appelo, 2013). Due to the consumption of CH_4 by sulfate reduction within the seal, we start from the assumption that the irreducible water film within the anhydrite seal equilibrates with a partial pressure of $CO_{2(g)}$ ($pCO_{2(g)}$), which is equal to the $pCO_{2(g)}$ in the gas cap. The pore water composition calculated for the gas cap is assumed to also prevail in the pore space of the GWT zone and of the water leg. Table S.3 summarizes the chemical composition of pore (or irreducible) water calculated for the different reservoir parts in equilibrium with the primary minerals and gases under the initial conditions. These calculated compositions (Table S.3) will be entered as input parameters in the input file of the computer code PHAST for the three-dimensional reactive mass transport modeling.

Appendix 2: Additional Modeling Results

The pH and pE values are the key variables characterizing the hydrogeochemical conditions in pore (or irreducible) water. Due to calcite precipitation and dolomite dissolution, the pH calculated in scenario 1–reference for 10 m.y. shows a small change compared with the initial conditions, although protons are produced and consumed in the ASR and thermochemical sulfate reduction (TSR) processes (Figure S.1). Water newly forms as one of the products of TSR (Figure S.1).

Due to the lack of data, several parameters are arbitrarily preassigned by assumed values. In order to test how these parameters affect the hydrogen sulfide (H_2S) concentration in the gas and the souring intensity, alternative scenarios vary the value of these parameters (e.g., tortuosity, rate constant of ASR, the initial mineralogical composition of the reservoir rocks). The H_2S produced by TSR is present in two forms in the reservoir: as free gas and as dissolved species in pore or irreducible water. Artificial effects on the produced fluids (e.g., changes in temperature and pressure due to fluid production from reservoirs) would result in H_2S outgassing from dissolved $S(-II)_{(aq)}$ species and consequently increase the H_2S concentration in the gas. Thus, the total concentration of S(–II) species ($H_2S_{(g)}$ + all $S(-II)_{(aq)}$ species dissolved in water) is one important parameter to evaluate the reservoir souring and consequently is defined as the reservoir souring intensity in our study. Due to presentation limitations, the spatial distribution of the H_2S concentration in the gas and of the souring intensity calculated from the alternative scenarios is presented in Supplementary Materials only for the time step of 10 m.y. (Figures S.2–S.4).

REFERENCES CITED

Dean, J. A., 1999, Lange's handbook of chemistry, 15th ed., New York, McGraw-Hill, p. 3.21–3.22, 3.33.

Parkhurst, D. L., and C. A. J. Appelo, 2013, Description of input and examples for PHREEQC Version 3—A computer program for speciation, batch-reaction, one-dimensional transport, and inverse geochemical calculations: US Geological Survey Techniques and Methods 6–A43, 497 p.

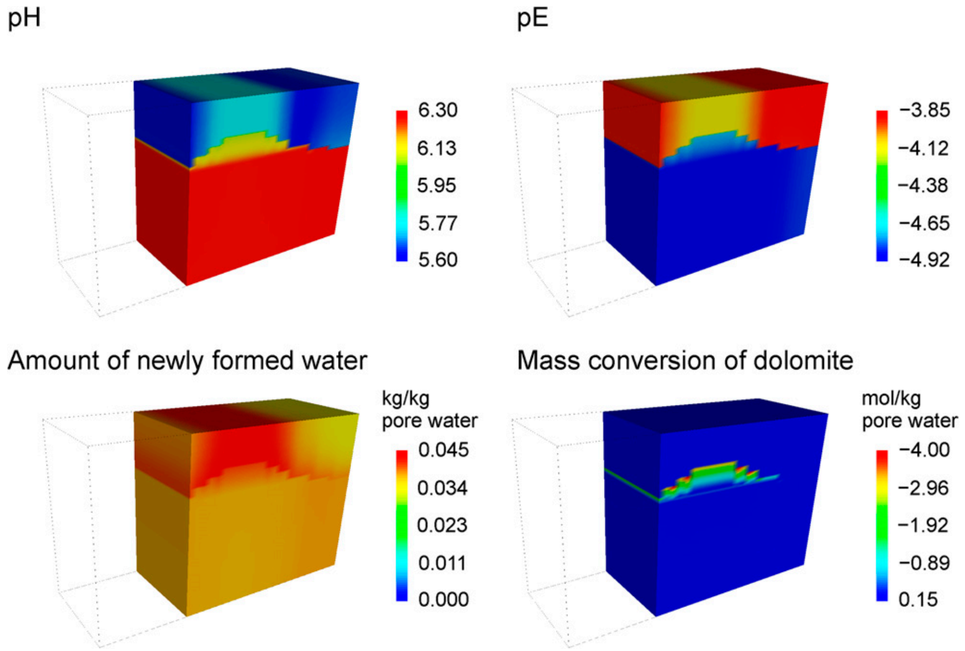

Figure S.1. Calculated spatial distribution of pH, pE, amount of newly formed water, and mass conversion of dolomite after 10 million years for scenario 1–reference. Positive or negative mass conversion of dolomite indicate precipitation or dissolution of dolomite, respectively.

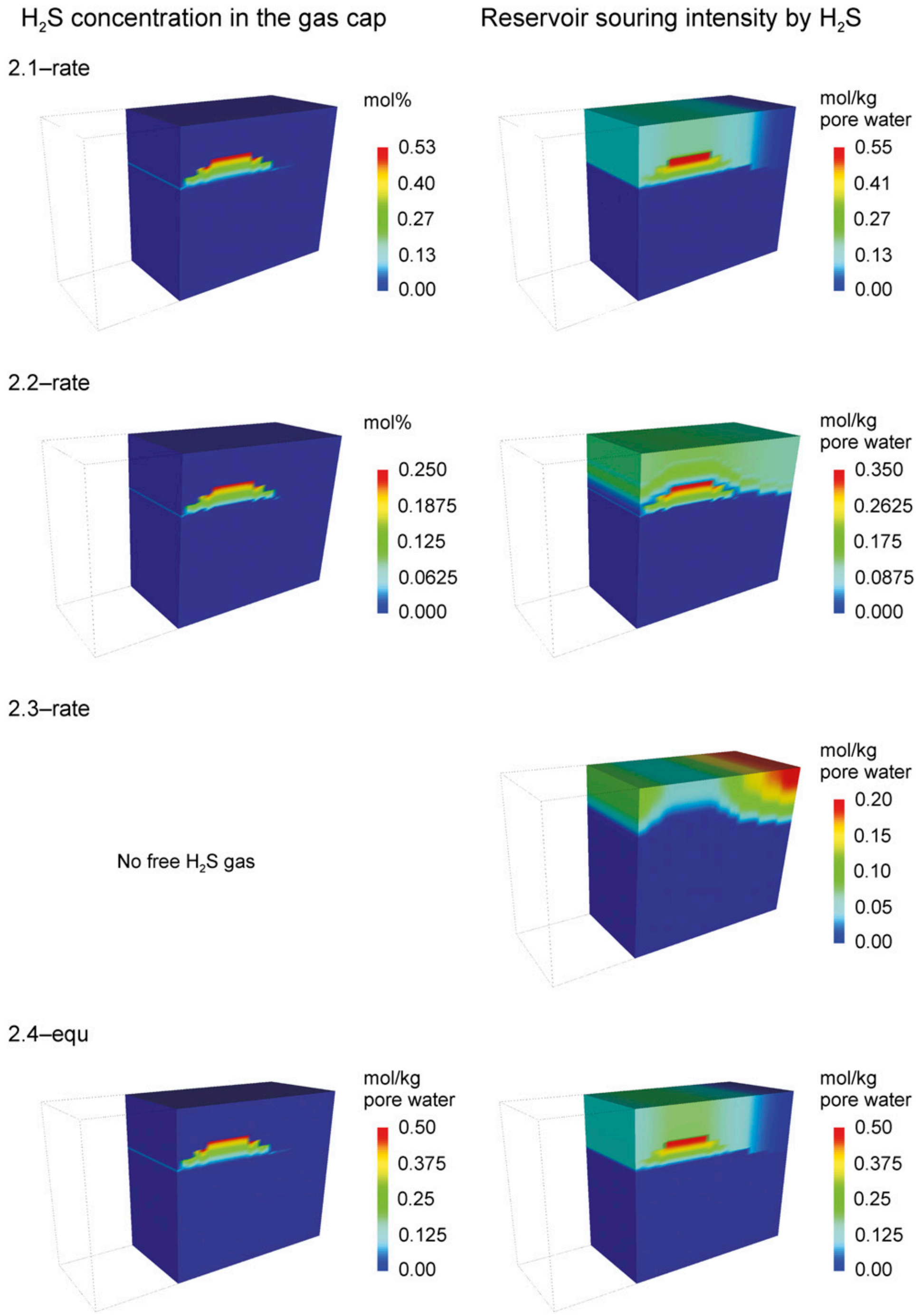

Figure S.2. Calculated spatial distribution of the hydrogen sulfide (H_2S) concentration in the gas and the reservoir souring intensity by H_2S (summed concentration of gaseous H_2S ($H_2S_{(g)}$), aqueous H_2S ($H_2S_{(aq)}$), aqueous bisulfide ($HS^{-}_{(aq)}$), aqueous sulfide ion ($S^{2-}_{(aq)}$), aqueous disulfide ion ($S_2{}^{2-}_{(aq)}$) to aqueous hexa-polysulfide ion ($S_6{}^{2-}_{(aq)}$), aqueous ferrous iron di-hydrogen sulfide complex ($Fe(HS)_{2(aq)}$), and aqueous ferrous iron tri-hydrogen sulfide complex ($Fe(HS)_3{}^{-}_{(aq)}$) after 10 million years for scenarios 2.1–rate, 2.2–rate, 2.3–rate, and 2.4–equ.

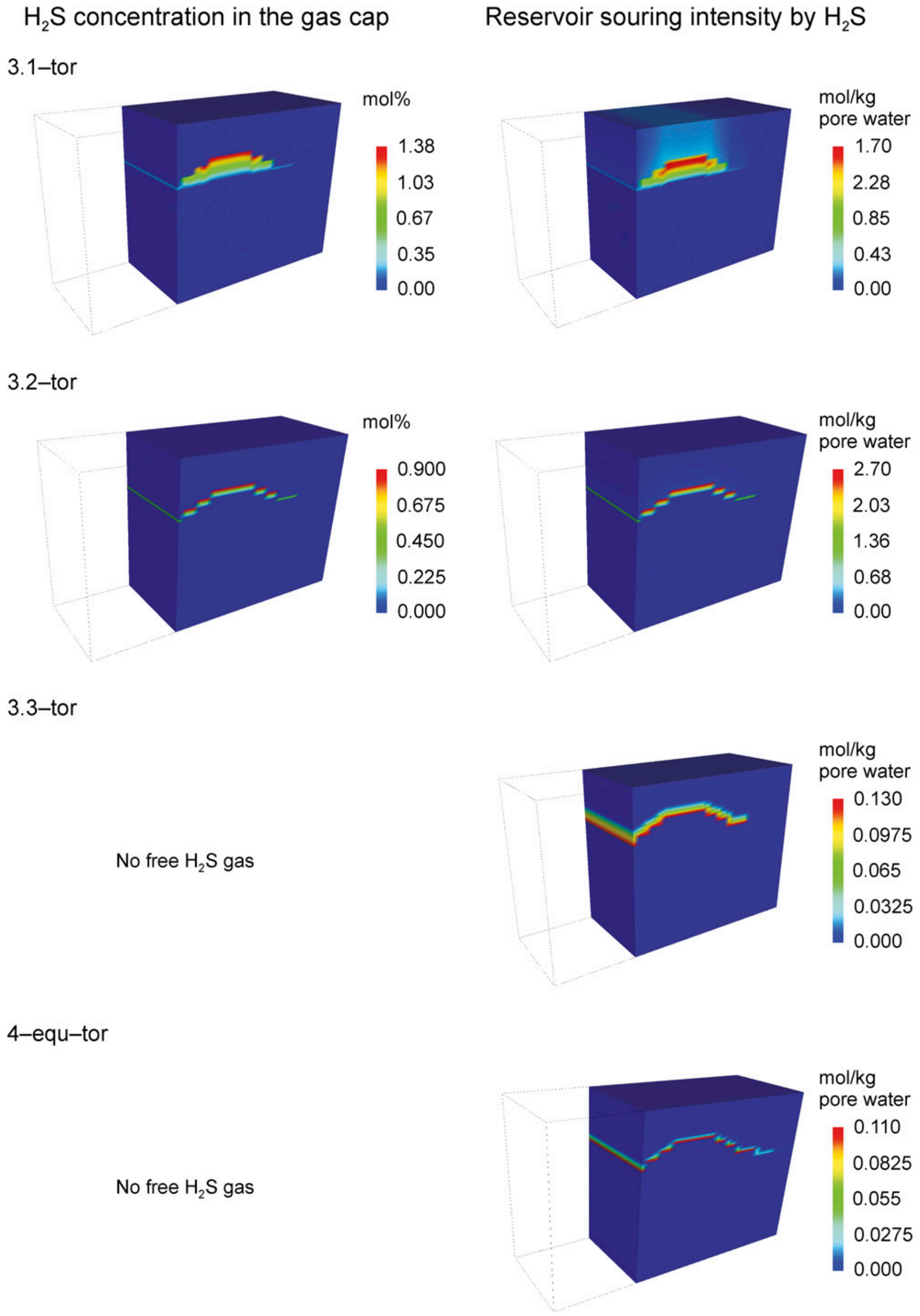

Figure S.3. Calculated spatial distribution of the hydrogen sulfide (H_2S) concentration in gas and the reservoir souring intensity by H_2S (summed concentration of gaseous H_2S ($H_2S_{(g)}$), aqueous H_2S ($H_2S_{(aq)}$), aqueous bisulfide ($HS^{-}{}_{(aq)}$), aqueous sulfide ion ($S^{2-}{}_{(aq)}$), aqueous disulfide ion ($S_2{}^{2-}{}_{(aq)}$) to aqueous hexapolysulfide ion ($S_6{}^{2-}{}_{(aq)}$), aqueous ferrous iron di-hydrogen sulfide complex ($Fe(HS)_{2(aq)}$), and aqueous ferrous iron tri-hydrogen sulfide complex ($Fe(HS)_3{}^{-}{}_{(aq)}$) after 10 million years for scenarios 3.1–tor, 3.2–tor, 3.3–rate, and 4–equ–tor.

Figure S.4. Calculated spatial distribution of the hydrogen sulfide (H_2S) concentration in the gas and the reservoir souring intensity by H_2S (summed concentration of gaseous H_2S ($H_2S_{(g)}$), aqueous H_2S ($H_2S_{(aq)}$), aqueous bisulfide ($HS^-_{(aq)}$), aqueous sulfide ion ($S^{2-}_{(aq)}$), aqueous disulfide ion ($S_2{}^{2-}_{(aq)}$) to aqueous hexapolysulfide ion ($S_6{}^{2-}_{(aq)}$), aqueous ferrous iron di-hydrogen sulfide complex ($Fe(HS)_{2(aq)}$), and aqueous ferrous iron tri-hydrogen sulfide complex ($Fe(HS)_3{}^-_{(aq)}$) after 10 million years for scenarios 5–without–S and 6–without–Goe.

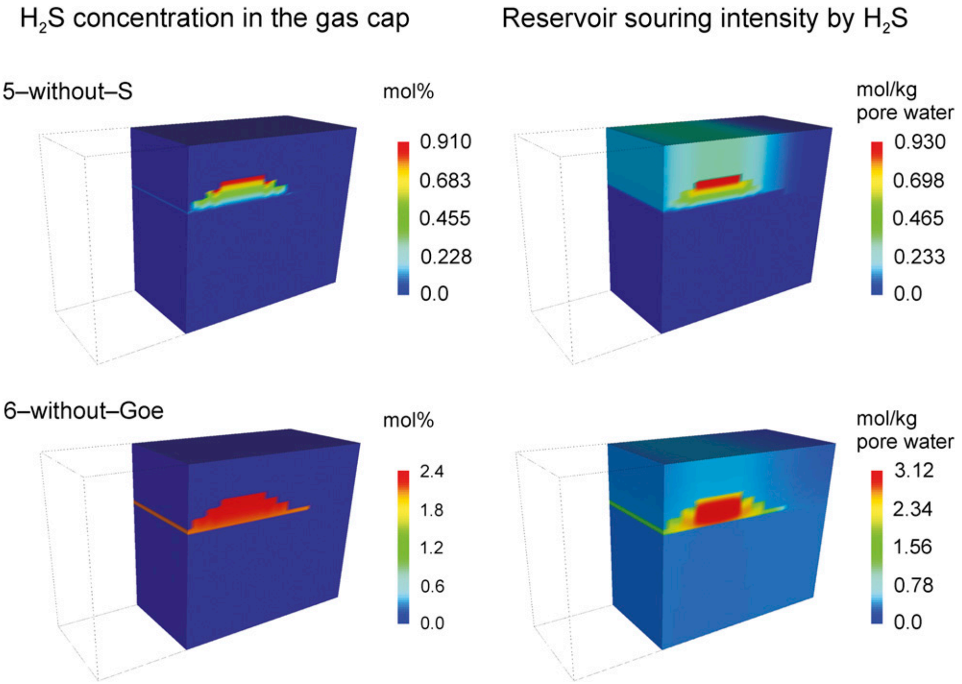

Table S.1. Semigeneric Reservoir Rock Properties for Scenario 1–Reference

Reservoir Unit	Thickness	Porosity (%)	Water Content (vol %)	Hydraulic Conductivity[†] (m s^{-1})	Dispersivity[‡]	Δh[§]	X	Y	Z	Tortuosity	Boundary Conditions for Diffusion
Seal	15–30 m (49–98 ft)	1	1*	1.0×10^{-8}	10.0; 1.0; 1.0 m (32.8; 3.3; 3.3 ft)	None	25 m (82 ft)	1 m (3.3 ft)	1 m (3.3 ft)	0.01	Open
Gas cap	2–12 m (7–39 ft)	10	1*	1.0×10^{-6}	10.0; 1.0; 1.0 m (32.8; 3.3; 3.3 ft)	None	25 m (82 ft)	1 m (3.3 ft)	1 m (3.3 ft)	0.1	Open
GWTZ	2–3 m (7–10 ft)	10	10	1.0×10^{-6}	10.0; 1.0; 1.0 m (32.8; 3.3; 3.3 ft)	None	25 m (82 ft)	1 m (3.3 ft)	1 m (3.3 ft)	0.5	Open
Water leg	50 m (164 ft)	10	10	1.0×10^{-6}	10.0; 1.0; 1.0 m (32.8; 3.3; 3.3 ft)	None	25 m (82 ft)	1 m (3.3 ft)	1 m (3.3 ft)	1.0	Open

Abbreviation: GWTZ = gas–water transition zone. X = cell length; Y = cell width; Z = cell height.

*Irreducible water content assumed (initial content before ASR onset).

[†] Assumed hydraulic conductivity$_{(x \text{ and } y)}$; hydraulic conductivity$_z$ = 0.1 times hydraulic conductivity$_{(x \text{ and } y)}$.

[‡] Longitudinal, horizontal, and vertical dispersivity values.

[§] Gradient of hydraulic head.

Table S.2. Initial Hydrogeochemical Conditions before ASR Onset for Scenario 1–Reference.

	Primary Mineral Assemblage								Gas Phase	
	Anhydrite		Calcite		Dolomite		Goethite			
Reservoir Unit	wt. %	mol/kgw	wt. %	mol/kgw	wt. %	mol/kgw	wt. %	mol/kgw	$p\text{CO}_{2(g)}$	$p\text{CH}_{4(g)}$
Seal	99.0	1973.6	1.0	26.0	n.p.		n.p.		18 atm (265 psi)	0 atm (15 psi)
Gas cap	n.p.		10.0	26.0	89.0	125.4	1.0	2.9	18 atm (265 psi)	582 atm (8552 psi)
GWTZ	n.p.		10.0	26.0	89.0	125.4	1.0	2.9	n.p.	n.p.
Water leg	n.p.		10.0	26.0	89.0	125.4	1.0	2.9	n.p.	n.p.

Abbreviations: GWTZ = gas–water transition zone; mol/kgw = mole per killigram pore water or killigram irreducible water; n.p. = not present as a primary phase or as a gas component; $p\text{CH}_{4(g)}$ = partial pressure of methane; $p\text{CO}_{2(g)}$ = partial pressure of carbon dioxide.

Table S.3. Calculated Chemical Composition of Pore (or Irreducible) Water in the Different Reservoir Parts in Equilibrium with the Primary Minerals and Gases under the Initial Conditions

Parameter	Seal	Reservoir Rock[‡]
Temperature	140°C (284°F)	140°C (284°F)
pH	5.399	5.967
pE	–0.028	–4.577
Unit*	mol/kgw	mol/kgw
Calcium	2.614e–2	3.223e–3
Carbon[†]	1.260e–1	3.454e–1
Chloride	1.500e–0	1.501e–0
Sodium	1.500e–0	1.501e–0
Sulfate	1.706e–2	n.p.
Iron	n.p.	1.735e–6
Magnesium	n.p.	1.847e–2

The calculated compositions apply to all modeling scenarios under initial conditions except for scenario 6–without–Goe in which the pore (or irreducible) water in the reservoir rocks is free of iron species.

Abbreviation: n.p. = not present.

*Unit of the total concentration of aqueous ions.

[†] Summed concentration of aqueous CH_4 and aqueous carbonate species.

[‡] Irreducible water calculated in equilibrium with the primary minerals and the gas of the gas cap (Table S.2); This water is also assumed to fill the pore space of the gas–water transition zone and of the water leg.

Table S.4. Calculated “Conditional” Equilibrium Constants of Minerals and Gases Involved in the Web of Chemical Reactions at 140°C (284°F) and 600 atm (8818 psi)

Consecutive Number	Minerals or Gases	Reaction	Log K (140°C [284°F] and 600 atm [8818 psi])*
1	Calcite	$CaCO_3 = CO_3^{2-} + Ca^{2+}$	−9.47
2	Dolomite	$CaMg(CO_3)_2 = Ca^{2+} + Mg^{2+} + 2CO_3^{2-}$	−18.07
3	Anhydrite	$CaSO_4 = Ca^{2+} + SO_4^{2-}$	−5.56
4	Elemental sulfur$_{(s)}$	$S + 2H^+ + 2e^- = H_2S$	2.66
5	Goethite	$FeOOH + 3H^+ = Fe^{3+} + 2H_2O$	−4.24
6	Pyrite	$FeS_2 + 2H^+ + 2e^- = Fe^{2+} + 2HS^-$	−16.40
7	Siderite	$FeCO_3 = CO_3^{2-} + Fe^{2+}$	−10.98
8	$CH_{4(g)}$	$CH_4 = CH_4$	−3.24
9	$CO_{2(g)}$	$CO_2 = CO_2$	−2.26
10	$H_2S_{(g)}$	$H_2S = H^+ + HS^-$	−8.19
11	$H_{2(g)}$	$H_2 = H_2$	−3.23

*Considering the ionic strength of a 1.5 molal NaCl aqueous solution at 140°C (284°F) and 600 atm (8818 psi); calculations applying the computer code PHREEQC Interactive 3.1.4–8929 and its thermodynamic phreeqc.dat database (Parkhurst and Appelo, 2013).

Table S.5. Equilibrium Reactions (49) for Aqueous Species Considered in the Model

Consecutive Number	Reaction and Aqueous Species$_{(aq)}$*
1	H2O = OH– + H+
2	2 H2O = O2 + 4 H+ + 4 e–
3	2 H+ + 2 e– = H2
4	CO3–2 + 10 H+ + 8 e– = CH4 + 3 H2O
5	CO3–2 + 2 H+ = CO2 + H2O
6	CO3–2 + H+ = HCO3–
7	Ca+2 + CO3–2 = CaCO3
8	Ca+2 + CO3–2 + H+ = CaHCO3+
9	Fe+2 + CO3–2 = FeCO3
10	Fe+2 + HCO3– = FeHCO3+
11	Mg+2 + CO3–2 = MgCO3
12	Mg+2 + H+ + CO3–2 = MgHCO3+
13	Ca+2 + SO4–2 = CaSO4
14	Ca+2 + HSO4– = CaHSO4+
15	Ca+2 + H2O = CaOH+ + H+
16	Mg+2 + SO4–2 = MgSO4
17	Mg+2 + H2O = MgOH+ + H+
18	Fe+2 = Fe+3 + e–
19	Fe+2 + H2O = FeOH+ + H+
20	Fe+2 + 3H2O = Fe(OH)3– + 3H+
21	Fe+2 + SO4–2 = FeSO4
22	Fe+2 + HSO4– = FeHSO4+
23	Fe+2 + 2HS– = Fe(HS)2
24	Fe+2 + 3HS– = Fe(HS)3–
25	Fe+3 + H2O = FeOH+2 + H+
26	Fe+3 + 2 H2O = Fe(OH)2+ + 2 H+
27	Fe+3 + 3 H2O = Fe(OH)3 + 3 H+
28	Fe+3 + 4 H2O = Fe(OH)4– + 4 H+
29	Fe+2 + 2H2O = Fe(OH)2 + 2H+
30	2 Fe+3 + 2 H2O = Fe2(OH)2+4 + 2 H+
31	3 Fe+3 + 4 H2O = Fe3(OH)4+5 + 4 H+
32	Fe+3 + SO4–2 = FeSO4+
33	Fe+3 + HSO4– = FeHSO4+2
34	Fe+3 + 2 SO4–2 = Fe(SO4)2–
35	SO4–2 + H+ = HSO4–
36	SO4–2 + 10 H+ + 8 e– = H2S + 4 H2O
37	HS– = S–2 + H+
38	HS– + H+ = H2S
39	HS– = S2–2 + H+[†]
40	HS– = S3–2 + H+[†]
41	HS– = S4–2 + H+[†]
42	HS– = S5–2 + H+[†]
43	HS– = S6–2 + H+[†]
44	Na+ + CO3–2 = NaCO3–
45	Na+ + HCO3– = NaHCO3
46	Na+ + SO4–2 = NaSO4–
47	Fe+3 + Cl– = FeCl+2
48	Fe+3 + 2Cl– = FeCl2+
49	Fe+3 + 3Cl– = FeCl3+

(*continued*)

Table S.5. Continued

*Original notation from the wateq4f.dat database (Parkhurst and Appelo, 2013); this database includes the equilibrium constant for 25°C (77°F) and 1 atm (15 psi) and its temperature dependence.

[†] Original expression taken from the wateq4f.dat database (Parkhurst and Appelo, 2013); the identifiers "-no_check" and "-mole_balance" of the codes PHAST and PHREEQC ensure a correct stoichiometry of the equations (for details, see Parkhurst and Appelo, 2013).